Received: 1 April 2022 | Revised: 21 June 2022 | Accepted: 24 June 2022

DOI: 10.1002/zamm.202200132

ORIGINAL PAPER

Some analytical solutions to peridynamic beam equations

Zhenghao Yang[1] | **Konstantin Naumenko**[2] | **Holm Altenbach**[2] | **Chien-Ching Ma**[1] | **Erkan Oterkus**[3] | **Selda Oterkus**[3]

[1]Department of Mechanical Engineering, National Taiwan University, Taipei, Taiwan

[2]Institute of Mechanics, Otto von Guericke University, Magdeburg, Germany

[3]PeriDynamics Research Centre, Department of Naval Architecture, Ocean and Marine Engineering, University of Strathclyde, Glasgow, UK

Correspondence
Zhenghao Yang, Department of Mechanical Engineering, National Taiwan University, Taipei, Taiwan.
Email: yangzh2006@hotmail.com

Peridynamics (PD) has been introduced to account for long range internal force/moment interactions and to extend the classical continuum mechanics (CCM). PD equations of motion are derived in the form of integro-differential equations and only few analytical solutions to these equations are presented in the literature. The aim of this paper is to present analytical solutions to PD beam equations for both static and dynamic loading conditions. Applying trigonometric series, general solutions for the deflection function are derived. For several examples in the static case including simply supported beam and cantilever beam, the coefficients in the series are presented in a closed analytical form. For the dynamic case, the solution is derived for a simply supported beam applying the variable separation with respect to the time and the axial coordinate. Several numerical cases are presented to illustrate the derived solutions. Furthermore, PD results are compared against results obtained from the classical beam theory (CBT). A very good agreement between these two different approaches is observed for the case of the small horizon sizes (HSs), which shows the capability of the current approach.

1 | INTRODUCTION

Peridynamics (PD) is a non-local theory, which operates with long-range force/moment interactions [1]. Unlike the classical continuum mechanics (CCM), the deformation gradient, its higher gradients or gradients of internal state variables are not introduced. PD equations of motion are integro-differential equations, in contrast to CCM where partial differential equations are introduced. This makes PD attractive in analysis of discontinuities such as cracks. Many numerical studies of complex fracture processes illustrate the ability of PD to capture crack initiation [2–4], crack branching [5], crack kinking [6] and crack interaction with initial heterogeneities, such as holes and pores [7, 8].

PD theories for components including rods and beams [9–13], plates [14–19] and shells [20–22] are developed. Within the CCM, these theories provide an efficient and robust approach for the analysis of structures. Indeed many analytical solutions for beams, plates and shells are available providing a direct insight into the deformation and stress states. On the other hand, they are useful to validate the numerical methods and computer codes, such as the finite element method. However, unlike the CCM, only few analytical solutions to PD equations are available.

Abbreviations: BC, boundary conditions; CBT, classical beam theory; CCM, classical continuum mechanics; PD, peridynamics.

This is an open access article under the terms of the Creative Commons Attribution License, which permits use, distribution and reproduction in any medium, provided the original work is properly cited.
© 2022 The Authors. *ZAMM - Journal of Applied Mathematics and Mechanics* published by Wiley-VCH GmbH.

Peristatic and PD solutions for one-dimensional rods are presented in Refs. [23–26]. For beams under static loading several truncated PD solutions are derived in Chen [9]. The deflection function is expanded in the Taylor series about a point of a beam. The PD integral equation for the bending moment is then evaluated approximately by keeping two terms of the series expansion. This approach leads to a non-local beam theory with higher derivatives of the unknown deflection function.

The aim of this study is to derive analytical solutions to PD beam equations for both static and dynamic loading conditions. By use of trigonometric series representation, general solutions for the deflection function are derived. For several boundary conditions in the static case and for a simply supported beam in the dynamic case, the coefficients in the series are evaluated in a closed analytical form. The results are validated by comparing against solutions to the classical beam theory (CBT).

2 | PERIDYNAMIC BEAM THEORY

2.1 | Equation of motion

The PD equation of motion for the Bernoulli–Euler beam can be derived by using Lagrange's equation

$$\frac{d}{dt}\frac{\partial L}{\partial \dot{w}} - \frac{\partial L}{\partial w} = 0 \tag{1}$$

where w is the deflection and $L = T - U$ represents the Lagrangian. The total kinetic energy, T, of the system can be written as follows:

$$T = \frac{1}{2}\int_0^L \rho A \dot{w}^2 \mathrm{d}x \tag{2}$$

in which ρ is the density, A is the cross sectional area and L is the length of the beam. The potential energy U is defined as follows:

$$U = \int_0^L W_{\mathrm{PD}}(x)\mathrm{d}x - \int_0^L p(x)w(x)\mathrm{d}x, \tag{3}$$

where W_{PD} is the PD strain energy density and $p(x)$ is the distributed transverse load.

PD as a non-local theory, whose strain energy density function has non-local form such that for any certain material point, it not only depends on its own deflection but also that of its finite neighbourhood. In order to obtain the PD strain energy density function, it can be achieved by converting the local term in corresponding strain energy density function in CBT into non-local form. For the Bernoulli–Euler beam, it takes the form

$$W_{CBT} = \frac{EI}{2}\left(w''\right)^2, \tag{4}$$

where E is the Young's modulus and I is the second moment of area of the beam cross section. Performing Taylor expansion on the displacement function about x and ignore the higher order terms results in

$$w(x+\xi) - w(x) = w'\big|_x \xi + \frac{1}{2} w''\big|_x \xi^2 \tag{5}$$

Considering x as a fixed point, multiplying each term in Equation (5) by $1/\xi^2$ and integrating over the PD domain gives

$$\begin{aligned} &\int_{-\delta}^{\delta} \frac{w(x+\xi)-w(x)}{\xi^2} d\xi = w'\big|_x \int_{-\delta}^{\delta} \frac{1}{\xi} d\xi + \frac{1}{2} w''\big|_x \int_{-\delta}^{\delta} d\xi = \delta\, w''\big|_x \\ &\Rightarrow w''(x) = \frac{1}{\delta}\int_{-\delta}^{\delta} \frac{w(x+\xi)-w(x)}{\xi^2} d\xi, \end{aligned} \tag{6}$$

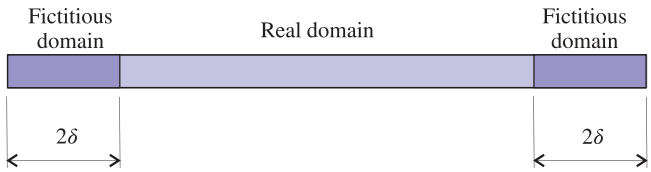

FIGURE 1 Real and fictitious domains for the beam

where δ is the finite size neighbourhood of the material point x, which is called the horizon. Note that the kernel function $1/\xi^2$ in Equation (6) ensures the dimension of the integrand to be consistent with that of curvature. Plugging Equation (6) back into Equation (4) arises the PD strain energy density as

$$W_{\mathrm{PD}} = \frac{EI}{2}\left[\frac{1}{\delta}\int_{-\delta}^{\delta}\frac{w(x+\xi)-w(x)}{\xi^2}d\xi\right]^2 \tag{7}$$

With Equations (2), (3) and (7), Equation (1) results in the following equation of motion [13]

$$\rho A\ddot{w} = c\int_{-\delta}^{\delta}\frac{1}{\xi^2}\left[\int_{-\delta}^{\delta}\frac{w(x+\eta)-w(x)}{\eta^2}d\eta - \int_{-\delta}^{\delta}\frac{w(x+\xi+\eta)-w(x+\xi)}{\eta^2}d\eta\right]d\xi + p(x), \quad c = \frac{EI}{\delta^2} \tag{8}$$

2.2 | Peridynamic boundary conditions

Equation of motion (8) is valid only if the material points are completely embedded in its PD influence domain. However, for material points adjacent to the boundary whose PD influence domain is defective, it is necessary to introduce fictitious material region for the sake of ensuring the validation of the PD formulation. In this study, the width of the fictitious region is suggested as the double of the PD HS, 2δ, as shown in Figure 1. Let us explain how to implement boundary supports in PD framework.

2.2.1 | Simple support

Suppose the beam is subjected to simply supported boundary condition at the left end. From geometrical point of view, the deflection and curvature of the end point must be zero, that is

$$\begin{cases} w(0) = 0, \\ \left.\dfrac{\mathrm{d}^2 w}{\mathrm{d}x^2}\right|_{x=0} = 0 \end{cases} \tag{9}$$

Applying the central difference for Equation $(9)_2$ yields

$$\left.\frac{\mathrm{d}^2 w}{\mathrm{d}x^2}\right|_{x=0} \approx \frac{w(-\Delta x) - 2w(0) + w(\Delta x)}{\Delta x^2} = 0 \tag{10}$$

Replacing Δx by ξ and associating with Equation $(9)_1$ gives the PD simply supported condition as

$$w(-\xi) = -w(\xi), \quad \text{for} \quad 0 \le \xi \le 2\delta \tag{11}$$

It indicates that simply supported end enforces in the fictitious region an anti-symmetric relation with respect to the real material domain, as shown in Figure 2.

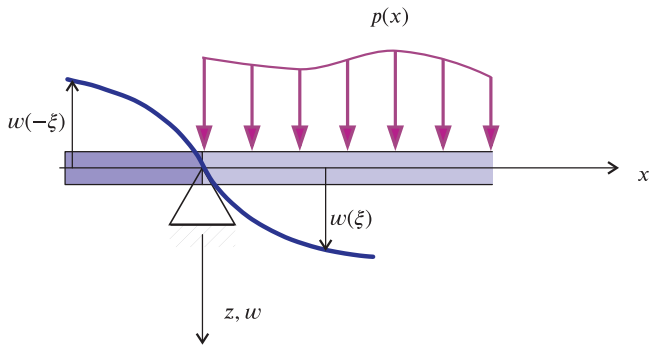

FIGURE 2 Simply supported beam with a fictitious region

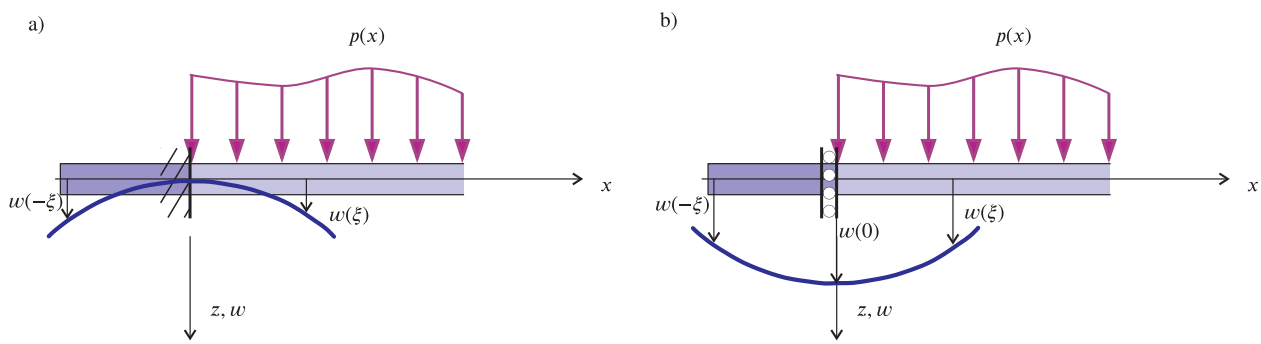

FIGURE 3 Clamped beam with a fictitious region

2.2.2 | Clamped support

Suppose the beam is clamped at the left end. In this case, both the deflection and cross section rotation must be zero, that is

$$\begin{cases} w(0) = 0, \\ \left.\dfrac{\mathrm{d}w}{\mathrm{d}x}\right|_{x=0} = 0 \end{cases} \tag{12}$$

Applying central difference with respect to the slope relation gives

$$\left.\frac{\mathrm{d}w}{\mathrm{d}x}\right|_{x=0} \approx \frac{w(\Delta x) - w(-\Delta x)}{2\Delta x} = 0 \tag{13}$$

Replacing Δx by PD notation ξ and associating with Equation $(12)_1$ gives the PD clamped boundary condition as

$$\begin{cases} w(0) = 0, \\ w(-\xi) = w(\xi) \end{cases} \qquad \text{for} \quad 0 \le \xi \le 2\delta \tag{14}$$

Equation (14) implies that clamped boundary in the fictitious region provides a symmetric relation with respect to the real material domain, as shown in Figure 3a.

Regarding roller clamped boundary (Figure 3b), Equation (14) reduces to

$$w(-\xi) = w(\xi) \qquad \text{for} \quad 0 \le \xi \le 2\delta \tag{15}$$

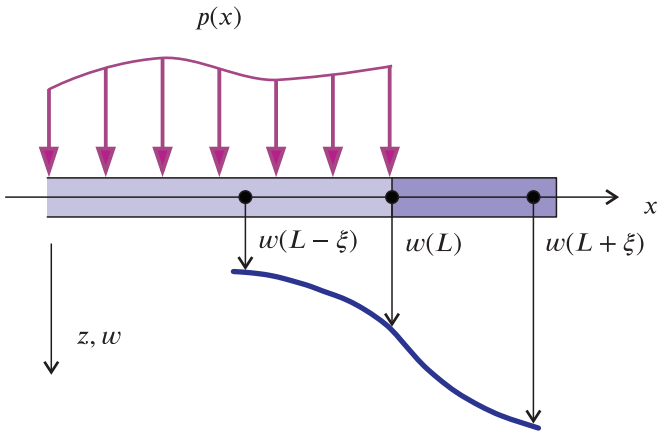

FIGURE 4 A beam with a free boundary

2.2.3 | Free boundary condition

The free boundary condition imposes both the zero curvature and shear force, that is

$$\begin{cases} \left.\dfrac{\mathrm{d}^2 w}{\mathrm{d}x^2}\right|_{x=L} = 0 \\ \left.\dfrac{\mathrm{d}^3 w}{\mathrm{d}x^3}\right|_{x=L} = 0 \end{cases} \tag{16}$$

Applying the central difference scheme with respect to zero curvature expression gives

$$\left.\frac{\mathrm{d}^2 w}{\mathrm{d}x^2}\right|_{x=L} \approx \frac{w(L-\Delta x) - 2w(L) + w(L+\Delta x)}{\Delta x^2} = 0 \quad \Rightarrow \quad w(L+\xi) = 2w(L) - w(L-\xi) \tag{17}$$

The central difference scheme applied to zero shear force gives

$$\begin{aligned} &\left.\frac{\mathrm{d}^3 w}{\mathrm{d}x^3}\right|_{x=L} \approx \frac{-w(L-2\Delta x) + 2w(L-\Delta x) - 2w(L+\Delta x) + w(L+2\Delta x)}{2\Delta x^3} = 0 \\ &\Rightarrow -w(L-2\xi) + 2w(L-\xi) - 2w(L+\xi) + w(L+2\xi) = 0 \end{aligned} \tag{18}$$

Coupling Equation (17) with Equation (18) yields

$$-w(L-2\xi) + 2w(L-\xi) - 2w(L+\xi) + w(L+2\xi) = -2w(L-2\xi) + 4w(L-\xi) - 2w(L) \approx -2\xi^2 \left.\frac{\mathrm{d}^2 w}{\mathrm{d}x^2}\right|_{x=L} \tag{19}$$

It can be claimed that the relation given in Equation (17) automatically satisfies zero shear force boundary conditions. Thus, the PD free boundary condition can be summarized as

$$w(L+\xi) = 2w(L) - w(L-\xi) \qquad \text{for} \quad 0 \le \xi \le 2\delta \tag{20}$$

In geometrical point of view, this enforces a skew symmetric relation about point $(x, z) = (L, w(L))$ between fictitious region and real material vicinal to free end, as shown in Figure 4.

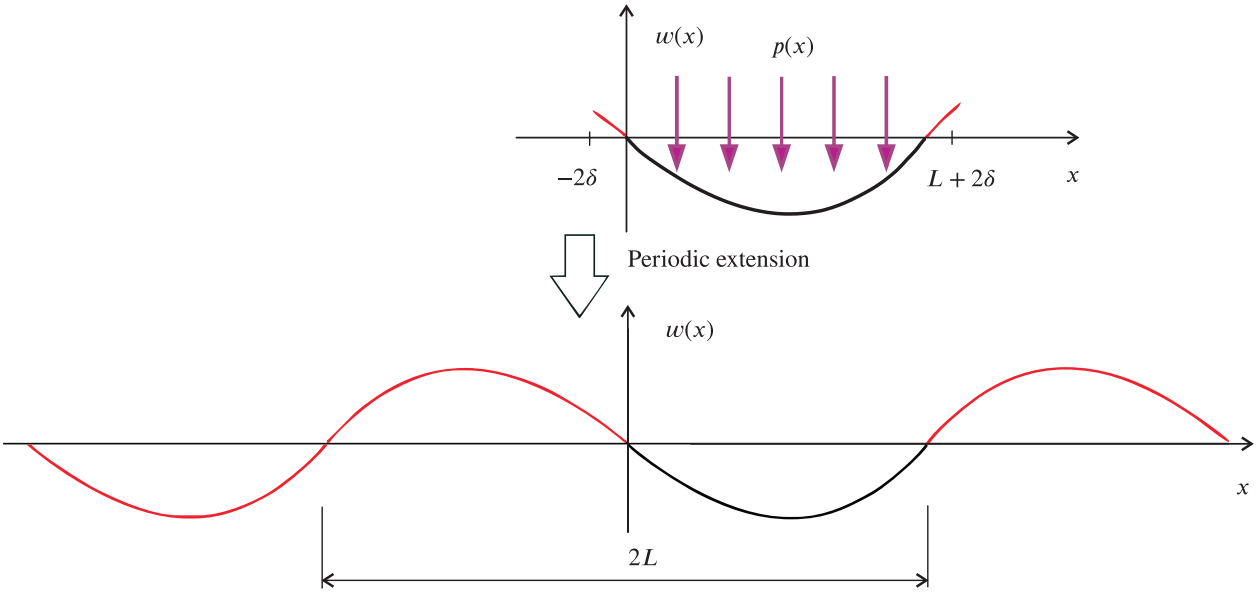

FIGURE 5 Periodic extension of the deflection line

3 | ANALYTICAL SOLUTIONS FOR BEAMS UNDER STATIC LOADING

3.1 | Simply supported beam

The PD governing equation for the Bernoulli–Euler beam (8) in the static case can be expressed as

$$c\int_{-\delta}^{\delta}\frac{1}{\xi^2}\left[\int_{-\delta}^{\delta}\frac{w(x+\eta)-w(x)}{\eta^2}d\eta-\int_{-\delta}^{\delta}\frac{w(x+\xi+\eta)-w(x+\xi)}{\eta^2}d\eta\right]d\xi=-p(x),\quad c=\frac{EI}{\delta^2} \tag{21}$$

with the following PD boundary conditions

$$w(-\xi)=-w(\xi),\quad w(L+\xi)=-w(L-\xi),\quad (0<\xi\le 2\delta) \tag{22}$$

The BCs (22) periodically extend the displacement field oddly with period of 2L, as shown in Figure 5.

With consideration of oddity and periodicity, the displacement field function can be expressed in terms of Fourier series as follows:

$$w(x)=\sum_{n=1}^{\infty}b_n\sin\frac{n\pi x}{L} \tag{23}$$

Consequently one may compute

$$\int_{-\delta}^{\delta}\frac{w(x+\eta)-w(x)}{\eta^2}d\eta=\sum_{n=1}^{\infty}b_n\int_{-\delta}^{\delta}\frac{1}{\eta^2}\left[\sin\frac{n\pi(x+\eta)}{L}-\sin\frac{n\pi x}{L}\right]d\eta \tag{24}$$

Likewise it follows:

$$\int_{-\delta}^{\delta}\frac{w(x+\xi+\eta)-w(x+\xi)}{\eta^2}d\eta=\sum_{n=1}^{\infty}b_n\sin\frac{n\pi(x+\xi)}{L}\int_{-\delta}^{\delta}\frac{1}{\eta^2}\left(\cos\frac{n\pi\eta}{L}-1\right)d\eta \tag{25}$$

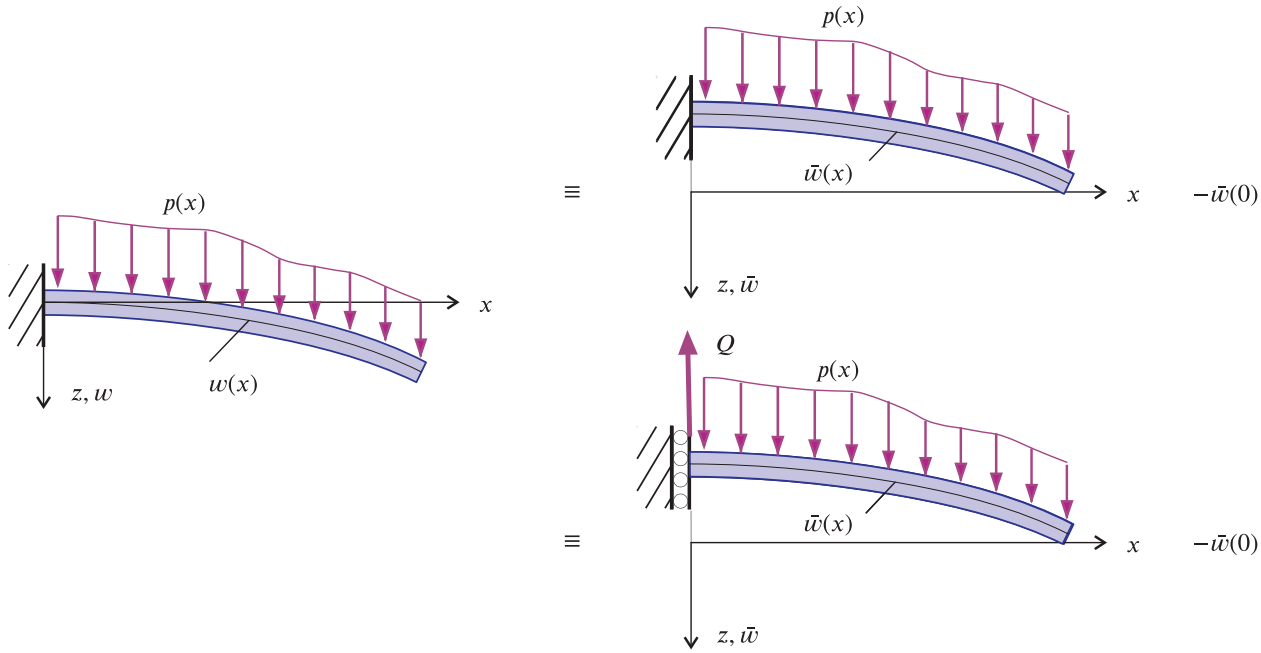

FIGURE 6 Solution decomposition for a cantilever beam

Plugging Equations (24) and (25) into Equation (21) and simplifying results in

$$c\sum_{n=1}^{\infty} b_n \sin\frac{n\pi x}{L}\left[\int_{-\delta}^{\delta}\frac{1}{\xi^2}\left(1-\cos\frac{n\pi\xi}{L}\right)d\xi\right]^2 = p(x) \tag{26}$$

Invoking trigonometric orthogonality implies

$$b_n = \frac{2}{Lc}\frac{\int_0^L p(x)\sin\frac{n\pi x}{L}dx}{\left[\int_{-\delta}^{\delta}\frac{1}{\xi^2}\left(1-\cos\frac{n\pi\xi}{L}\right)d\xi\right]^2} \tag{27}$$

Plugging Equation (27) into Equation (23) gives the PD analytical solution for the simply supported beam as follows:

$$w(x) = \frac{2}{Lc}\sum_{n=1}^{\infty}\frac{\int_0^L p(x)\sin\frac{n\pi x}{L}dx}{\left[\int_{-\delta}^{\delta}\frac{1}{\xi^2}\left(1-\cos\frac{n\pi\xi}{L}\right)d\xi\right]^2}\sin\frac{n\pi x}{L} \tag{28}$$

3.2 | Cantilever beam

Suppose a cantilever beam subjected to arbitrary load, the solution to cantilever beam can be identically decomposed by following process (Figure 6):

1. Transit the origin to level with the free end then subtract the corresponding rigid body motion
2. Release the vertical displacement constrain and replace it by the corresponding shear force Q

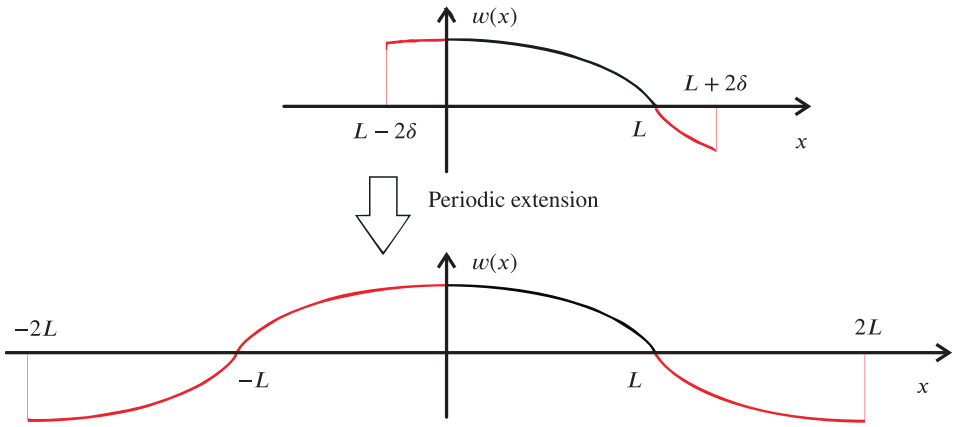

FIGURE 7 Periodic extension of the deflection line

Denote the solution to the original configuration as $w(x)$ and new configuration as $\overline{w}(x)$, respectively. Apparently, we have the following relation

$$w(x) = \bar{w}(x) - \bar{w}(0) \tag{29}$$

The PD governing equation for the new configuration becomes

$$c\int_{-\delta}^{\delta}\frac{1}{\xi^2}\left[\int_{-\delta}^{\delta}\frac{\bar{w}(x+\eta)-\bar{w}(x)}{\eta^2}d\eta - \int_{-\delta}^{\delta}\frac{\bar{w}(x+\xi+\eta)-\bar{w}(x+\xi)}{\eta^2}d\eta\right]d\xi = -p(x) - \Delta(x-0)Q, \quad c = \frac{EI}{\delta^2} \tag{30}$$

where $\Delta(x-0)$ represents the Dirac Delta function, and the shear force Q can be casted as

$$Q = -\int_0^L p(x)dx \tag{31}$$

The corresponding PD boundary conditions are

$$\begin{cases} \bar{w}(-\xi) = \bar{w}(\xi), \\ \bar{w}(L+\xi) = 2\bar{w}(L) - \bar{w}(L-\xi) \end{cases} \quad \text{for} \quad 0 \le \xi \le 2\delta \tag{32}$$

Based on the PD boundary stipulation in Equation (32), $\overline{w}(x)$ can be evenly extended with period of $4L$, as shown in Figure 7.

Thus, $\overline{w}(x)$ can be expressed by using Fourier series as follows:

$$\bar{w}(x) = \sum_{n=1}^{\infty} a_n \cos\left(\frac{n\pi x}{2L}\right) \tag{33}$$

Substitute Equation (33) into PD BC $(32)_2$ gives

$$\begin{aligned} &\bar{w}(L+\xi) + \bar{w}(L-\xi) - 2\bar{w}(L) = 0 \\ &\Rightarrow \sum_{n=1}^{\infty} a_n\left[\cos\frac{n\pi}{2L}(L+\xi) + \cos\frac{n\pi}{2L}(L-\xi) - 2\cos\frac{n\pi}{2}\right] = 0 \\ &\Rightarrow \sum_{n=1}^{\infty} a_n \cos\frac{n\pi}{2}\left(\cos\frac{n\pi\xi}{2L} - 1\right) = 0 \end{aligned} \tag{34}$$

Equation (34) identically holds if $n = 1,\ 3,\ 5,\ \ldots$ and Equation (33) thus reduces to

$$\bar{w}(x) = \sum_{n=1}^{\infty} a_{2n-1} \cos \frac{(2n-1)\pi x}{2L} \tag{35}$$

With Equation (35), we obtain

$$\int_{-\delta}^{\delta} \frac{\bar{w}(x+\eta) - \bar{w}(x)}{\eta^2} d\eta = \sum_{n=1}^{\infty} a_{2n-1} \int_{-\delta}^{\delta} \frac{1}{\eta^2} \left\{ \cos \frac{(2n-1)\pi(x+\eta)}{2L} - \cos \frac{(2n-1)\pi x}{2L} \right\} d\eta \tag{36}$$

Likewise it follows

$$\int_{-\delta}^{\delta} \frac{w(x+\xi+\eta) - w(x+\xi)}{\eta^2} d\eta = \sum_{n=1}^{\infty} a_{2n-1} \cos \frac{(2n-1)\pi(x+\xi)}{2L} \int_{-\delta}^{\delta} \frac{1}{\eta^2} \left\{ \cos \frac{(2n-1)\pi\eta}{2L} - 1 \right\} d\eta \tag{37}$$

Plugging Equations (36) and (37) into Equation (30) gives

$$\begin{aligned}
-\Delta(x-0)Q - p(x) &= c \int_{-\delta}^{\delta} \frac{1}{\xi^2} \left[\int_{-\delta}^{\delta} \frac{w(x+\eta) - w(x)}{\eta^2} d\eta - \int_{-\delta}^{\delta} \frac{w(x+\xi+\eta) - w(x+\xi)}{\eta^2} d\eta \right] d\xi \\
&= c \sum_{n=1}^{\infty} a_{2n-1} \int_{-\delta}^{\delta} \frac{1}{\eta^2} \left[\cos \frac{(2n-1)\pi\eta}{2L} - 1 \right] d\eta \int_{-\delta}^{\delta} \frac{1}{\xi^2} \left[\cos \frac{(2n-1)\pi x}{2L} - \cos \frac{(2n-1)\pi(x+\xi)}{2L} \right] d\xi \\
&= c \sum_{n=1}^{\infty} a_{2n-1} \int_{-\delta}^{\delta} \frac{1}{\eta^2} \left[\cos \frac{(2n-1)\pi\eta}{2L} - 1 \right] d\eta \int_{-\delta}^{\delta} \frac{1}{\xi^2} \left[1 - \cos \frac{(2n-1)\pi\xi}{2L} \right] d\xi \cos \frac{(2n-1)\pi x}{2L} \\
&= -c \sum_{n=1}^{\infty} a_{2n-1} \left\{ \int_{-\delta}^{\delta} \frac{1}{\xi^2} \left[\cos \frac{(2n-1)\pi\xi}{2L} - 1 \right] d\xi \right\}^2 \cos \frac{(2n-1)\pi x}{2L}
\end{aligned} \tag{38}$$

in which the Fourier series coefficients can be obtained as

$$a_{2n-1} = \frac{2}{cL} \frac{\int_0^L [p(x) + \Delta(x-0)Q] \cos \frac{(2n-1)\pi x}{2L} dx}{\left\{ \int_{-\delta}^{\delta} \frac{1}{\xi^2} \left[\cos \frac{(2n-1)\pi\xi}{2L} - 1 \right] d\xi \right\}^2} \tag{39}$$

Plugging Equation (39) back into Equation (35) implies

$$\bar{w}(x) = \frac{2}{cL} \sum_{n=1}^{\infty} \frac{\int_0^L [p(x) + \Delta(x-0)Q] \cos \frac{(2n-1)\pi x}{2L} dx}{\left\{ \int_{-\delta}^{\delta} \frac{1}{\xi^2} \left[\cos \frac{(2n-1)\pi\xi}{2L} - 1 \right] d\xi \right\}^2} \cos \frac{(2n-1)\pi x}{2L} \tag{40}$$

Substituting Equation (40) into Equation (29) results in the PD solution for cantilever beam as

$$w(x) = \frac{2}{cL} \sum_{n=1}^{\infty} \frac{\int_0^L [p(x) + \Delta(x-0)Q] \cos \frac{(2n-1)\pi x}{2L} dx}{\left\{ \int_{-\delta}^{\delta} \frac{1}{\xi^2} \left[\cos \frac{(2n-1)\pi\xi}{2L} - 1 \right] d\xi \right\}^2} \left(\cos \frac{(2n-1)\pi x}{2L} - 1 \right) \tag{41}$$

in which

$$Q = -\int_0^L p(x)dx, \quad c = \frac{EI}{\delta^2} \tag{42}$$

4 | ANALYTICAL SOLUTION FOR FREE VIBRATION OF SIMPLY SUPPORTED BEAM

By using variable separation method, the displacement function can be expressed as

$$w(x,t) = X(x)T(t) \tag{43}$$

After inserting Equation (43) into Equation (8), we obtain

$$c\int_{-\delta}^{\delta}\frac{1}{\xi^2}\left[\int_{-\delta}^{\delta}\frac{X(x+\eta)T(t)-X(x)T(t)}{\eta^2}d\eta-\int_{-\delta}^{\delta}\frac{X(x+\xi+\eta)T(t)-X(x+\eta)T(t)}{\eta^2}d\eta\right]d\xi = \rho A X(x)\ddot{T}(t) \tag{44}$$

By isolating variables, it follows

$$\frac{1}{X(x)}\int_{-\delta}^{\delta}\frac{1}{\xi^2}\left[\int_{-\delta}^{\delta}\frac{X(x+\eta)-X(x)}{\eta^2}d\eta-\int_{-\delta}^{\delta}\frac{X(x+\xi+\eta)-X(x+\eta)}{\eta^2}d\eta\right]d\xi = \frac{\rho A}{c}\frac{\ddot{T}(t)}{T(t)} = -\lambda \tag{45}$$

Thus, we obtain

$$\int_{-\delta}^{\delta}\frac{1}{\xi^2}\left[\int_{-\delta}^{\delta}\frac{X(x+\eta)-X(x)}{\eta^2}d\eta-\int_{-\delta}^{\delta}\frac{X(x+\xi+\eta)-X(x+\eta)}{\eta^2}d\eta\right]d\xi = -\lambda X(x) \tag{46}$$

and

$$\frac{\rho A}{c}\ddot{T}(t) + \lambda T(t) = 0 \tag{47}$$

By comparing Equation (46) with Equation (21), we can consider $X(x)$ as an analogue to $w(x)$ and $\lambda X(x)$ to $p(x)/c$. Thus, associating with Equations (23) and (26), one can obtain

$$X(x) = \sum_{n=1}^{\infty} b_n \sin\frac{n\pi x}{L} \tag{48}$$

and

$$\sum_{n=1}^{\infty} b_n \sin\frac{n\pi x}{L}\left[\int_{-\delta}^{\delta}\frac{1}{\xi^2}\left(1-\cos\frac{n\pi\xi}{L}\right)d\xi\right]^2 = \sum_{n=1}^{\infty}\lambda_n b_n \sin\frac{n\pi x}{L} \tag{49}$$

Therefore, the PD eigenvalue can be casted as

$$\lambda_n = \left[\int_{-\delta}^{\delta}\frac{1}{\xi^2}\left(1-\cos\frac{n\pi\xi}{L}\right)d\xi\right]^2 \tag{50}$$

The general solution to Equation (47) can be expressed as

$$T_n(t) = A_n^* \cos\left(\sqrt{\lambda_n\frac{c}{\rho A}}t\right) + B_n^* \sin\left(\sqrt{\lambda_n\frac{c}{\rho A}}t\right) \tag{51}$$

With Equations (48) and (51), the general PD solution can be formulated as follows:

$$w(x,t)=\sum_{n=1}^{\infty}\left[A_n\cos\left(\sqrt{\lambda_n\frac{c}{\rho A}}t\right)+B_n\sin\left(\sqrt{\lambda_n\frac{c}{\rho A}}t\right)\right]\sin\frac{n\pi x}{L},\quad A_n=A_n^*b_n,\quad B_n=B_n^*b_n \tag{52}$$

in which the undetermined coefficients A_n and B_n depend upon the initial conditions. Suppose the initial conditions are

$$\begin{cases} w(x,0)=w_0(x)\\ \dot{w}(x,0)=v_0(x)\end{cases} \tag{53}$$

By associating Equation (52), we have

$$w_0(x)=\sum_{n=1}^{\infty}A_n\sin\frac{n\pi x}{L} \tag{54}$$

and

$$v_0(x)=\sum_{n=1}^{\infty}\sqrt{\lambda_n\frac{c}{\rho A}}B_n\sin\frac{n\pi x}{L} \tag{55}$$

Utilizing orthogonal properties gives

$$A_n=\frac{2}{L}\int_0^L w_0(x)\sin\frac{n\pi x}{L}dx,\quad B_n=\frac{2}{L}\frac{1}{\sqrt{\lambda_n\frac{c}{\rho A}}}\int_0^L v_0(x)\sin\frac{n\pi x}{L}dx \tag{56}$$

By collecting derivation above, the PD analytic solution for free vibration of Euler beam can be summarized as

$$\begin{aligned} &w(x,t)=\sum_{n=1}^{\infty}\left[A_n\cos\left(\sqrt{\lambda_n\frac{c}{\rho A}}t\right)+B_n\sin\left(\sqrt{\lambda_n\frac{c}{\rho A}}t\right)\right]\sin\frac{n\pi x}{L},\\ &A_n=\frac{2}{L}\int_0^L w_0(x)\sin\frac{n\pi x}{L}dx,\quad B_n=\frac{2}{L}\frac{1}{\sqrt{\lambda_n\frac{EI}{\delta^2\rho A}}}\int_0^L v_0(x)\sin\frac{n\pi x}{L}dx,\quad \lambda_n=\left[\int_{-\delta}^{\delta}\frac{1}{\xi^2}\left(1-\cos\frac{n\pi\xi}{L}\right)d\xi\right]^2 \end{aligned} \tag{57}$$

5 | NUMERICAL RESULTS

In order to demonstrate the validation of the PD analytical solution, various numerical cases are presented comparing against analytical solution in CBT for both static and dynamic condition. Different boundary conditions are considered including simply supported beam and cantilever beam.

5.1 | Static solution

Consider a beam with length of $L = 1$ m, thickness of $h = 0.01$ m, width of $b = 0.05$ m and Young's modulus of $E = 200$ GPa subjected to simply supported and clamped free boundary condition, respectively. The PD HS is chosen as $\delta = 0.001$ m. A distributed loading of $p(x) = 1$ N/m is applied for both cases, as shown in Figure 8a,b.

The variation of deflection along the beam from PD is calculated and compared against CCM solution. As shown in Figure 9a,b, a very good agreement is observed between PD and CBT solutions.

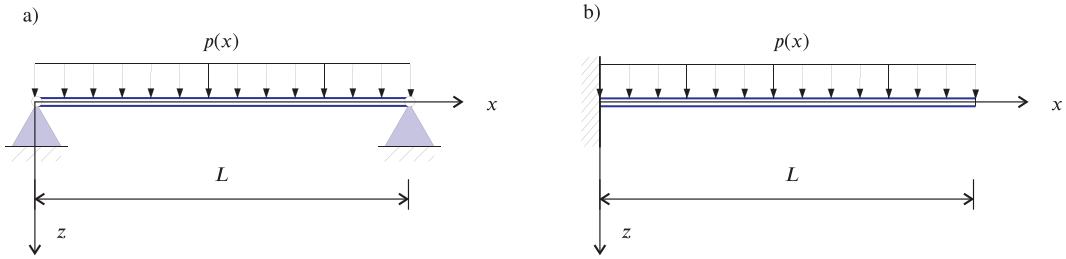

FIGURE 8 Examples for static solutions. (a) Simply supported beam, (b) cantilever beam

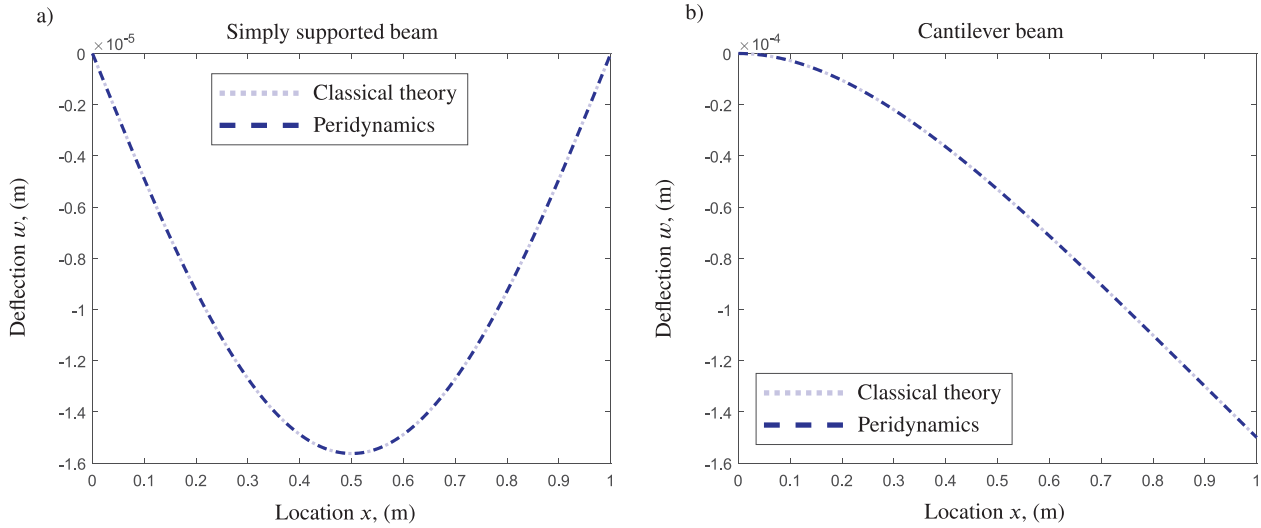

FIGURE 9 Deflection versus axial location under static loading. (a) Simply supported beam, (b) cantilever beam

5.2 | Free vibration

Consider a simply supported beam with dimensions of $L \times h \times b = 1\text{ m} \times 0.05\text{ m} \times 0.01\text{ m}$, Young's modulus and material density of $E = 200$ GPa and $\rho = 7850\text{ kg/m}^3$, respectively. The PD HS is chosen as $\delta = 0.001$ m. Initial conditions are specified as

$$w_0(x) = 0.001x(x-1)^2, \quad v_0(x) = 0 \tag{58}$$

The variation of deflection from PD analytical solution is obtained at two different locations $x = 0.25$ m and $x = 0.5$ m. As shown in Figure 10, a very good agreement is obtained between PD and CBT solutions.

5.3 | Analysis of PD horizon size effect

The horizon as an important parameter in PD, which is considered as a length-scale parameter and gives non-local property to the system. The size of the PD horizon determines the non-locality of the PD governing equation. If the size is chosen tending to zero, the PD solution should converge to that of CBT. It can be seen from Equation (57) that the natural frequencies obtained by PD solution are depended upon the HS δ. In order to investigate the effect of HS, vibrational behaviour of simply supported beam with various of hHS are compared against the corresponding solution in CBT.

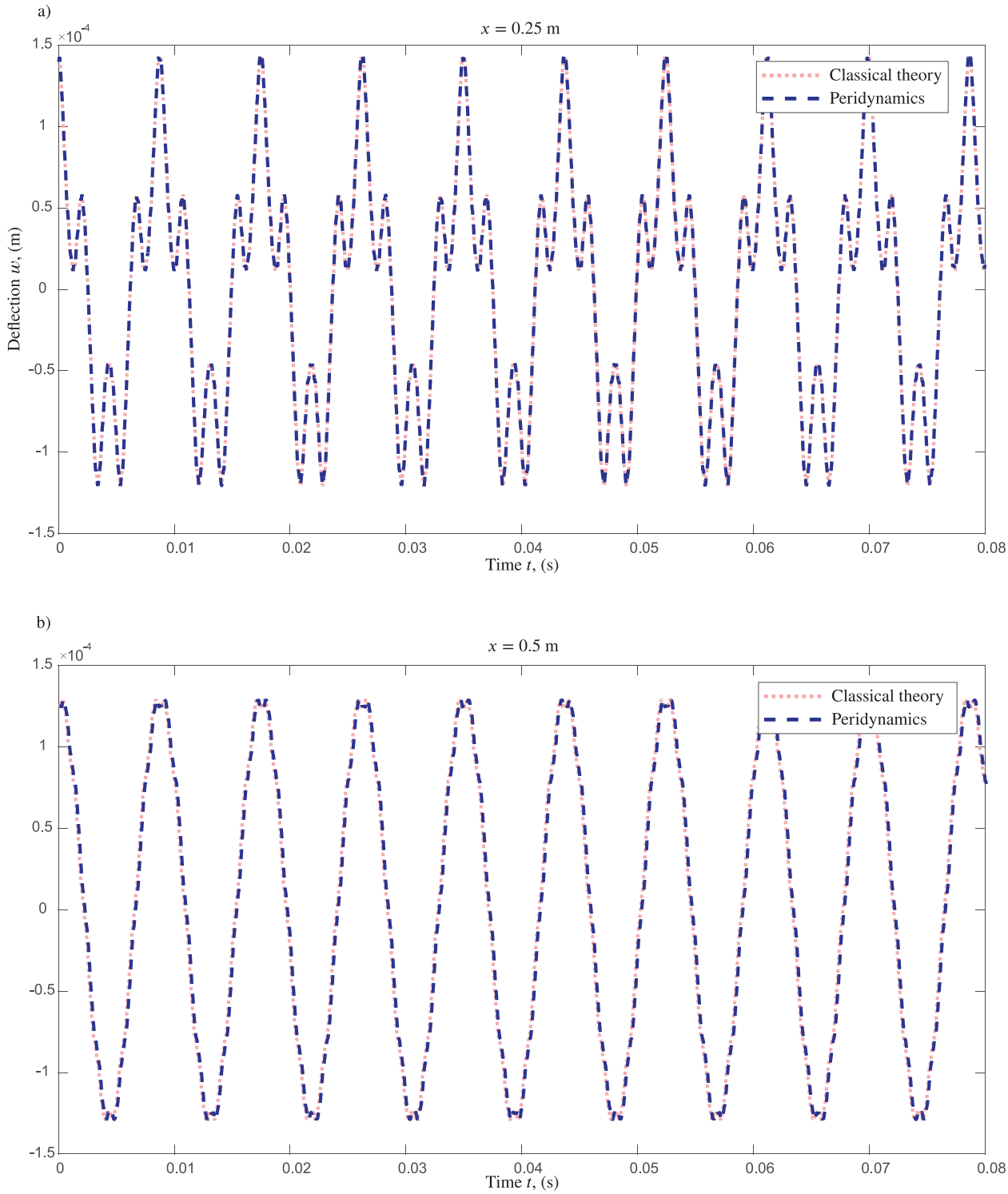

FIGURE 10 Deflection versus time for a simply supported beam. (a) $x = 0.25$ m, (b) $x = 0.5$ m

The geometric dimension of the beam is chosen as $L \times h \times b = 1\ \text{m} \times 0.05\ \text{m} \times 0.01\ \text{m}$ and the Young's modulus and material density are chosen as $E = 200$ GPa and $\rho = 7850\ \text{kg/m}^3$. The initial conditions are subjected as

$$\begin{cases} w_0(x) = 0.01x^2(1-x)(3x-2), \\ v_0(x) = 3\sin\left(\dfrac{\pi x}{L}\right) + 5\sin\left(\dfrac{2\pi x}{L}\right) \end{cases} \tag{59}$$

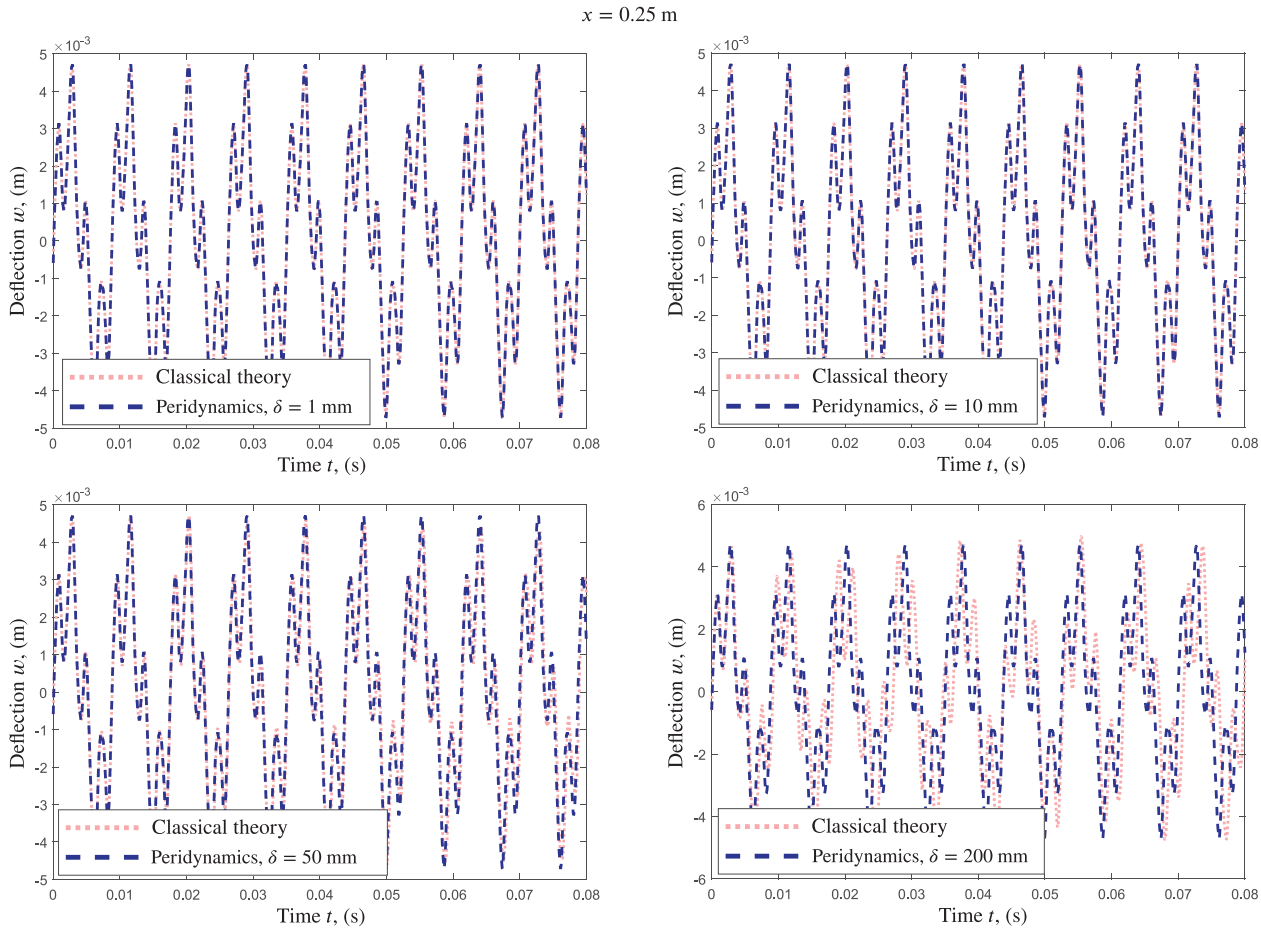

FIGURE 11 Deflection versus time for a simply supported beam for different horizon sizes and $x = 0.25$ m

Four HSs of $\delta = 1$ mm, $\delta = 10$ mm, $\delta = 50$ mm and $\delta = 200$ mm are considered, respectively. Two vibrational trajectories of material points at $x = 0.25$ m and $x = 0.5$ are selected as references and compared against CBT solution.

A very good agreement is observed between PD and CBT when the HSs are small, as illustrated in Figures 11 and 12. Let us note that as the HS approaches zero, the non-locality disappears and equations of the CBT follow from the PD beam equations. However, as the HS increases, solutions of PD diverge from CBT solution.

6 | CONCLUSIONS

In this study, new closed-form analytical solutions to PD beam equations are presented. By the use of trigonometric series, representation of the deflection function of the axial coordinate general solutions for the static case is derived. For several examples including simply supported beam and cantilever beam, the coefficients in the series are presented in a closed analytical form. For the dynamic case, the solution is derived for a simply supported beam. By the use of the variable separation, the deflection is represented as a function of the time and the axial coordinate. Numerical examples are presented to illustrate and to compare results of PD against solutions according to the CBT. A very good agreement between these two different approaches is observed for the case of the small HSs, which shows the capability of the current approach.

The derived analytical solutions can be applied in the future to verify the numerical methods and codes to solve PD equations.

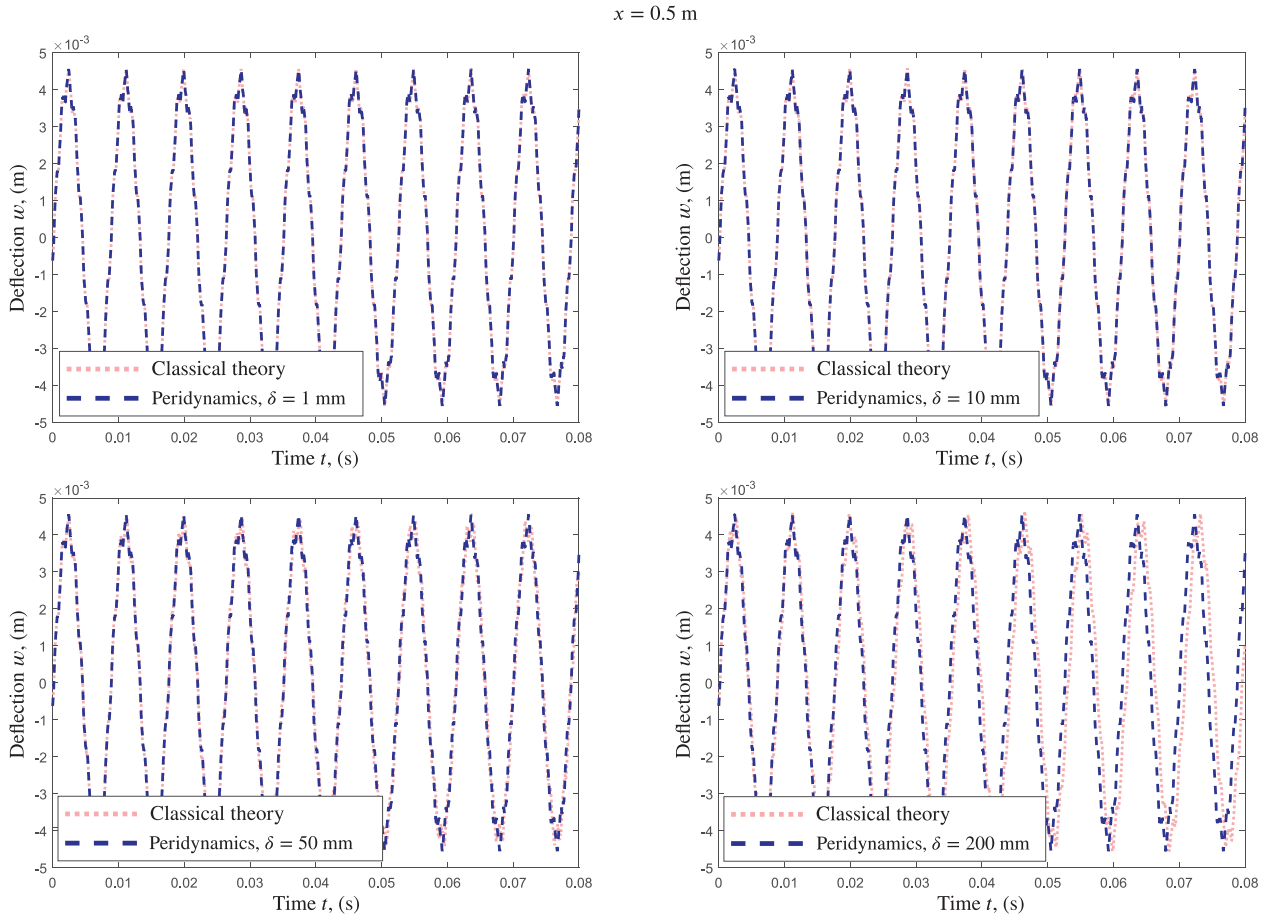

FIGURE 12 Deflection versus time for a simply supported beam for different horizon sizes and $x = 0.5$ m

ACKNOWLEDGEMENT

Open access funding enabled and organized by Projekt DEAL.

CONFLICT OF INTEREST

The authors have declared no conflict of interest.

ORCID

Konstantin Naumenko https://orcid.org/0000-0001-6072-0809
Holm Altenbach https://orcid.org/0000-0003-3502-9324

REFERENCES

[1] Silling, S.A., Lehoucq, R.B.: Peridynamic theory of solid mechanics. Adv. Appl. Mech. 44, 73–168 (2010)
[2] Naumenko, K., Pander, M., Würkner, M.: Damage patterns in float glass plates: Experiments and peridynamics analysis. Theor. Appl. Fract. Mech. 118, 103264 (2022)
[3] Niazi, S., Chen, Z., Bobaru, F.: Crack nucleation in brittle and quasi-brittle materials: A peridynamic analysis. Theor. Appl. Fract. Mech. 112, 102855 (2021)
[4] Wang, Z., Ma, D., Suo, T., Li, Y., Manes, A.: Investigation into different numerical methods in predicting the response of aluminosilicate glass under quasi-static and impact loading conditions. Int. J. Mech. Sci. 196, 106286 (2021)
[5] Mehrmashhadi, J., Bahadori, M., Bobaru, F.: On validating peridynamic models and a phase-field model for dynamic brittle fracture in glass. Eng. Fract. Mech. 240, 107355 (2020)
[6] Diana, V., Ballarini, R.: Crack kinking in isotropic and orthotropic micropolar peridynamic solids. Int. J. Solids Struct. 196, 76–98 (2020)
[7] Rahimi, M.N., Kefal, A., Yildiz, M., Oterkus, E.: An ordinary state-based peridynamic model for toughness enhancement of brittle materials through drilling stop-holes. Int. J. Mech. Sci. 182, 105773 (2020)

[8] Zhang, Y., Deng, H., Deng, J., Liu, C., Yu, S.: Peridynamic simulation of crack propagation of non-homogeneous brittle rock-like materials. Theor. Appl. Fract. Mech. 106, 102438 (2020)
[9] Chen, J.: Nonlocal Euler–Bernoulli Beam Theories: A Comparative Study. Springer, Cham (2021)
[10] Dorduncu, M.: Int. J. Mech. Sci. 185, 105866 (2020)
[11] Dorduncu, M.: Theor. Appl. Fract. Mech. 112, 102832 (2021). https://doi.org/10.1016/j.tafmec.2020.102832
[12] Moyer, E.T., Miraglia, M.J.: Peridynamic solutions for Timoshenko beams. Engineering 6, 304–317 (2014)
[13] Yang, Z., Oterkus, E., Oterkus, S.: A state-based peridynamic formulation for functionally graded Euler-Bernoulli beams. CMES-Comput. Model. Eng. Sci. 124(2), 527–544 (2020)
[14] Dorduncu, M., Kaya, K., Ergin, O.F.: Int. J. Appl. Mech. 12(03), 2050031 (2020). https://doi.org/10.1142/S1758825120500313
[15] Naumenko, K., Eremeyev, V.A.: A non-linear direct peridynamics plate theory. Compos. Struct. 279, 114728 (2022)
[16] Nguyen, C.T., Oterkus, S.: Ordinary state-based peridynamics for geometrically nonlinear analysis of plates. Theor. Appl. Fract. Mech. 112, 102877 (2021)
[17] Yang, Z., Vazic, B., Diyaroglu, C., Oterkus, E., Oterkus, S.: A Kirchhoff plate formulation in a state-based peridynamic framework. Math. Mech. Solids 25(3), 727–738 (2020)
[18] Yang, Z., Oterkus, E., Oterkus, S.: A state-based peridynamic formulation for functionally graded Kirchhoff plates. Math. Mech. Solids 26(4), 530–551 (2021)
[19] Yang, Z., Oterkus, E., Oterkus, S.: Peridynamic modelling of higher order functionally graded plates. Math. Mech. Solids 26(12), 1737–1759 (2021)
[20] Chowdhury, S.R., Roy, P., Roy, D., Reddy, J.N.: A peridynamic theory for linear elastic shells. Int. J. Solids Struct. 84, 110–132 (2016)
[21] Nguyen, C.T., Oterkus, S.: Peridynamics for the thermomechanical behavior of shell structures. Eng. Fract. Mech. 219, 106623 (2019)
[22] Shen, G., Xia, Y., Li, W., Zheng, G., Hu, P.: Modeling of peridynamic beams and shells with transverse shear effect via interpolation method. Comput. Methods Appl. Mech. Eng. 378, 113716 (2021)
[23] Mikata, Y.: Analytical solutions of peristatic and peridynamic problems for a 1d infinite rod. Int. J. Solids Struct. 49(21), 2887–2897 (2012)
[24] Nishawala, V.V., Ostoja-Starzewski, M.: Peristatic solutions for finite one- and two-dimensional systems. Math. Mech. Solids 22(8), 1639–1653 (2017)
[25] Silling, S.A., Zimmermann, M., Abeyaratne, R.: Deformation of a peridynamic bar. J. Elast. 73(1), 173–190 (2003)
[26] Weckner, O., Abeyaratne, R.: The effect of long-range forces on the dynamics of a bar. J. Mech. Phys. Solids 53(3), 705–728 (2005)

How to cite this article: Yang, Z., Naumenko, K., Altenbach, H., Ma, C.-C., Oterkus, E., Oterkus, S.: Some analytical solutions to peridynamic beam equations. Z. Angew. Math. Mech. e202200132 (2022). https://doi.org/10.1002/zamm.202200132